Catalyst-Support Interactions Promoted Acidic Electrochemical Oxygen Evolution Catalysis

Subjects: Chemistry, Applied

Contributor: Zijie Luo , Jia Wang , Wei Zhou , Junsheng Li

In the context of the growing human demand for green secondary energy sources, proton-exchange membrane water electrolysis (PEMWE) is necessary to meet the high-efficiency production of high-purity hydrogen required for proton-exchange membrane fuel cells (PEMFCs). The development of stable, efficient, and low-cost oxygen evolution reaction (OER) catalysts is key to promoting the large-scale application of hydrogen production by PEMWE.

fuel cell water electrolysis catalyst support interactions oxygen evolution

1. Introduction

Due to the non-renewable nature of fossil fuels, excessive consumption of fossil fuels for energy is bound to cause serious ecological problems [1]. According to a report by the International Energy Agency (IEA), total global energy demand will exceed the equivalent of 18 billion tonnes of oil by 2030 [2]. Therefore, the development of secondary energy is crucial to meet the needs of sustainable development. The need for efficient production of renewable, non-polluting secondary energy is also urgent to meet people's quest for a higher standard of living while preserving the ecological environment. Recently, renewable energy systems such as solar power, wind and tidal energy are considered as potential green secondary energy. However, the large-scale application of these energy conversion devices has been hindered by the limitations of their geographical nature, periodicity and high cost of long-distance transmission [3][4][5].

As a power generation device, proton-exchange membrane fuel cells (PEMFCs) have attracted various attention. PEMFCs can efficiently convert the chemical energy of hydrogen and oxygen directly into electrical energy [6]. On the other hand, PEMFCs have lower energy losses and higher energy conversion efficiencies because they do not need to go through the Carnot cycle to convert energy [7]. On the other hand, PEMFCs also have the advantage of zero missions, as the only running product is pure water. The raw material required for the PEMFCs is high-purity hydrogen. Oetjen et al. found that for Pt-based catalysts in PEMFCs, even if exposed to feed gas containing 100 ppm CO for 5 min, the catalytic performance would significantly decline [8]. Currently, conventional hydrogen production processes are still based on natural gas reforming. However, hydrogen obtained through the natural gas reforming process could not meet the standard required for PEMFCs application, due to its poor purity [2][9]. It would also be impractical to purify the hydrogen, which would add to the cost of production. The purity of hydrogen produced by proton-exchange membrane water electrolysis (PEMWE) is up to 99.99%, which has obvious

advantages over other hydrogen production methods [10]. Therefore, for PEMFCs to be deployed on a large scale, the promotion of PEMWE is of great importance.

The hydrogen produced by PEMWE is an ideal source of feed gas for the large-scale production of PEMFCs. PEMWE has the advantages of compact design, small footprint, high current density [11][12]. In practice, noble metals like Ir and Ru catalysts are heavily used in the OER catalysts designed to lower the potential barrier, leading to the high cost of PEMWE. According to the report, the cost of hydrogen production with PEMWE is as high as ~$10.30/kg, and only ~4% of the hydrogen is produced through PEMWE, due to the high cost [13]. Therefore, it is of great significance to design cost-effective, efficient and highly stable OER catalysts.

2. Fundamentals and Current Status of Research on Acidic OER

Although the O_2 produced by the OER reaction is a by-product of the electrolysis of water for hydrogen production, the reaction kinetics are slower in an acidic environment due to the fact that OER is a four-electron process and requires higher energy to overcome the high potential barrier of the kinetics [14]. As a result, the anode reaction consumes the most energy process in the entire electrolytic water process. In order to reduce the overpotential, large amounts of precious metal are used in the anode catalysts. Ir-based and Ru-based catalysts exhibit impressive catalytic activity for OER reactions in acidic media [15]. It is now generally accepted that the acidic OER process is dominated by two mechanistic routes, the adsorbed evolution mechanism (AEM) and lattice oxygen mechanism (LOM) [16]. As shown in **Figure 1**b, the OER process through AEM involves four steps and proceeds on a single adsorption site. There is a linear relationship between the adsorption energies of O*, *OH and *OOH [17]. Utilizing isotopic labelling, researchers have investigated the contribution of lattice oxygen to OER. The results show that the acidic OER process is co-dominated by both AEM and LOM. The proportion of LOM is related to the catalyst structure [18][19]. The LOM process typically has a lower activation barrier than the AEM process. However, the LOM process can lead to degradation of the active component of the catalyst, resulting in reduced stability of the OER catalyst [16][20].

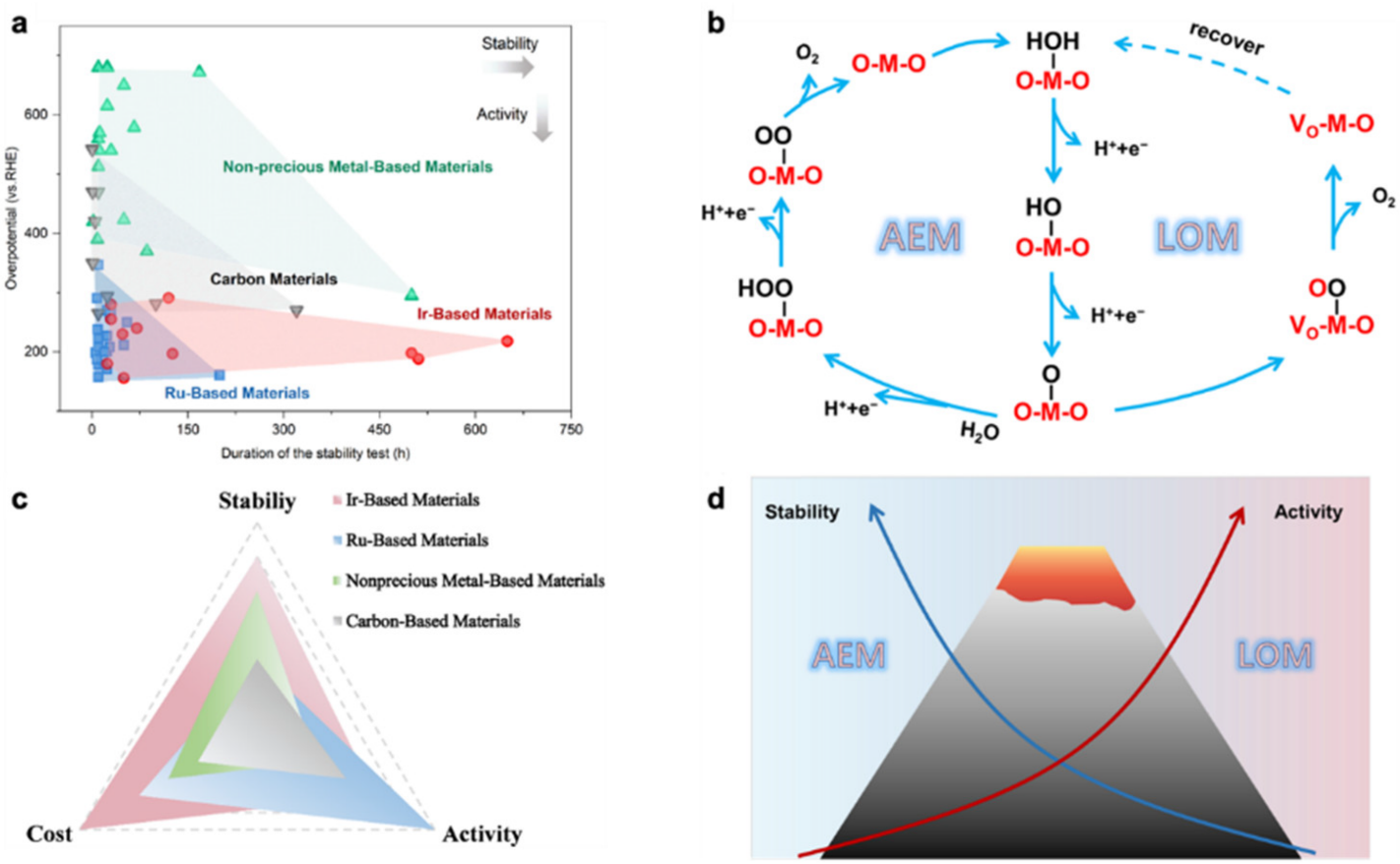

Figure 1. (**a**) Stability test time and ŋ10 of catalysts reported in recent years and (**b**) acid OER reaction mechanism. (**c**) The stability, activity, and cost of Ir-, Ru-, nonprecious metal-, and carbon-based materials. (**d**) Schematic diagram of the difference in stability and activity of the AEM/LOM mechanism [17].

Ir and Ru are noble metals, which is the main cost of electrolytic cells. This has become the biggest obstacle to the industrialization of PEMWE. However, in acidic media and under high-voltage conditions, both Ru-based and Ir-based catalysts are not sufficiently stable [21][22][23], which is not sufficient for the large-scale application of PEMWE. Great efforts have been made to improve the atomic utilization of precious metals and to enhance the performance and stability of acidic OER catalysts. Ru/Mo_2C heterojunctions were constructed to regulate the valence of Ru and Mo in the catalyst to simultaneously boost OER and HER in acidic conditions [24]. A chemical etching strategy for fabricating a Ru/Fe oxide towards OER resulted in enhanced stability [25]. Sr–Ru–Ir ternary oxide electrocatalysts: The electronic structure of active Ru sites was modulated by Sr and Ir, resulting in an overpotential of 190 mV at 10 mA cm^{-2}, and the overpotential remained below 225 mV following 1500 h of operation [23]. Rh-Ir alloy NPs prepared by a scalable microwave-assisted method with improved atom utilisation through ~10 nm ultra-fine size: Owing to the synergy of ensemble and electronic effects by alloying a small amount of Rh with Ir, the binding energy difference of the O and OOH intermediates was reduced, leading to faster kinetics and enhanced OER activity [26].

It has also been shown that alloys [27][28][29], perovskite material [30][31][32][33], single-atomic materials [34][35][36][37], MOF materials [38][39][40][41], and transition metal oxides [42][43] have potential applications in acidic OER.

Unfortunately, as is shown in **Figure 1**c, due to the harsh acidic conditions, it seems difficult to accomplish the balance of stability and catalytic performance with these reported non-precious metal catalysts. Therefore, the current position of noble metal catalysts in OER catalysts is still unshakable. Due to the high cost of noble metals, improving catalytic activity and durability of catalysts while reducing the amount of noble metals is the focus of current research. To further improve the industrial viability of PEMWE, researchers have explored many strategies that can significantly enhance the catalytic activity and stability of Ru-based and Ir-based catalysts for OER in acidic media, such as doping [44][45][46], morphological engineering [47][48], defect engineering [49][50], etc.

3. Support-Catalyst Interactions in Acidic OER

3.1. Metal Support Interaction (MSI)

MSI is commonly found in supported metal-based catalysts. Metal NPs are a fundamental component of various catalysts due to their unique electronic structure, morphology and controlled composition. Immobilization of metal NPs on support could improve their stability and control their spatial distribution. In addition, since carriers are usually not inert, the interaction between carriers and metal NPs can generate specific interfacial phenomena [51].

3.1.1. Charge Transfer

Due to the difference in Fermi energy levels between metal NPs and supports, interfacial contact between NPs and supports can induce changes in the electronic structure of both supports and NPs to seek an equilibrium in the electrochemical potential, and such changes are bi-directional in nature [52]. The metallic properties of the NPs give the electrons mobility. However, the mobility is related to the nanosystem because the smaller the NP, the more localized its electronic state is. In some cases, the charge transfer may be accompanied by a change in the oxidation state of the NPs or the metal ions of the supports [53].

3.1.2. Interfacial Perimeter

The interfacial region around the NPs forms a unique environment as the NPs, support and reactants make direct contact and synchronously promote the catalytic reaction. As a result, it can significantly enhance the adsorption and reactions of molecules at the perimeter [54]. The close proximity of NPs to different groups or defects (e.g., oxygen vacancies, hydroxyl groups, Lewis acids or Lewis bases) on the surface of the support may also contribute to localized sequential reactions of reactants or products, or the stabilization of transition states [38]. While this phenomenon of MSI can modulate the intensity of oxygenated intermediates adsorption by the catalyst, it accelerates the kinetics of the catalyst's reaction to the OER process.

3.1.3. Nanoparticle Morphology

The shape and crystal structure of NPs have a strong influence on their catalytic performance. This is because NPs of different morphologies expose distinct crystalline facets, which can result in either favorable or unfavorable atomic configurations in different reactions. Therefore, the activity and selectivity of catalysts can be effectively modulated by modulating the morphology of NPs at the metal-support interface [55]. Supported iridium- and

ruthenium-based NPs are potential OER catalysts for PEMWE, but the inhomogeneous dispersion of these NPs on the support and their inhomogeneous size usually leads to migration and adhesion of the catalyst at high potentials and strong acidity. Ultimately, this leads to a loss of active surface area and catalytic material, resulting in reduced OER performance.

3.1.4. Chemical Composition

Solid-state reactions can occur between the metal NPs and the support, resulting in the formation of a new phase. The exchange of species is possible in both directions and is usually designed for redox reactions [55]. The local composition of alloyed metal NPs can be affected by interactions with the support, where the rearrangement of components in alloyed NPs is driven by the interaction of their elements with the support at the interface. This can lead to compositional rearrangements that differ from the initial homogeneous composition, such as sub-nanostructures like core-shells, affecting the synergy between the metal and metal active sites and thus, their catalytic performance (**Figure 2**) [56].

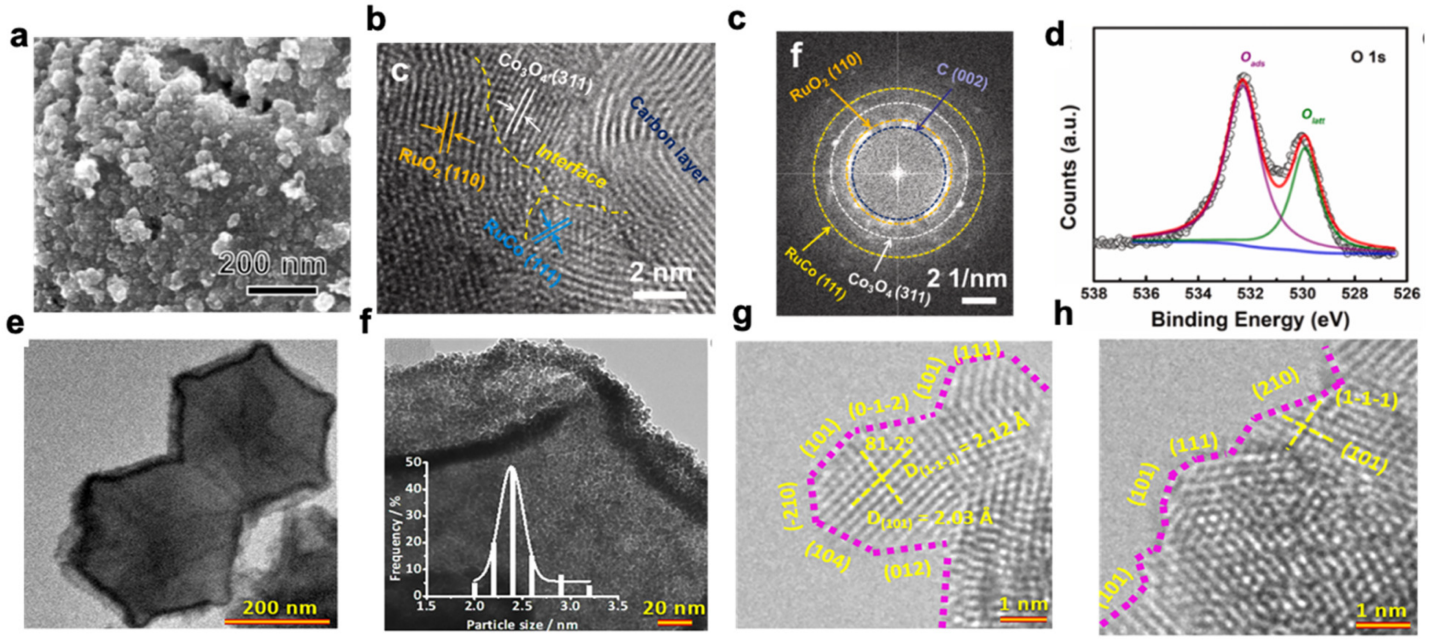

Figure 2. (**a**) SEM images of $RuCoO_x$-RuCo-NC; (**b**) line profiles of $RuCoO_x$-RuCo-NC; (**c**) HAADF-STEM elemental mappings; (**d**) XPS spectra of $RuCoO_x$-RuCo-NC: O 1s [54]; (**e**) SEM image of RuIr@CoNC catalysts; (**f**) size distribution of RuIr nanocrystals; (**g**,**h**) HRTEM images. Atomic steps are indicated with pink dotted lines [57].

3.2. Strong Metal-Support Interaction (SMSI)

Although SMSI is also an MSI phenomenon, because it has special characteristics compared to the other four common MSI phenomena, it will be discussed separately. SMSI was first proposed by Tauster et al. in 1978 [56]. Since then, researchers have conducted in-depth studies on the formation mechanism of SMSI, and it is generally agreed that one of the main reasons for the formation of SMSI is the different surface energy and work functions between metal NPs and supports, which drive the surface migration of the supports to the metal NPs, thus

stabilizing the metal NPs [55]. SMSIs are normally differentiated according to the different construction methods. SMSIs constructed using high temperature reduction are referred to as classical SMSIs [56]; those constructed with an oxygen atmosphere are referred to as O-SMSIs [58]; and those formed using adsorbent induction are referred to as A-SMSIs [59]. Although there are various methods of SMSI construction, there is still a lack of effective methods to purposefully construct SMSI on some relatively inert oxide supports such as SiO_2, CaO, Al_2O_3 and so on [60]. The use of SMSI can effectively modulate the distribution, valence, and ligand structure and stability of NPs on the surface of the support, creating great opportunities for the electronic structure modulation of the active component of the catalyst [60]. Xu et al. synthesized a series of M-Ru/RuO_2@CNT (M = Mn, Cd, Cu) bifunctional OER/HER catalysts. The OER activity and stability of the catalysts were improved by strong SMSI. The optimized Mn-Ru/RuO_2@CNT catalyst with an ultra-small particle size of 2.5 nm showed the best catalytic performance, with a low overpotential of 177 mV and 30 mV for OER and HER, respectively, at a current density of 10 mA cm^{-2} in 0.5 M H_2SO_4 [61].

(1) The migration of the support to the surface of the metal particles to form an inclusion structure. Zhang et al. constructed a classical SMSI by high temperature treatment of Au/TiO_2. The presence of an amorphous inclusion layer was observed by HETEM and the chemical components of the inclusion layer were analyzed by EELS [62]. The inclusion layer acted as immobilization and protection for the NPs. In the A-SMSI constructed in Rh/TiO_2, the Rh NPs were wrapped by amorphous TiO_x and the inclusions were composed of Ti species of different valence states (Ti^{3+}/Ti^{4+}=3/7), whereas in the Rh/TiO_2 catalyst with classical SMSI effect, the Rh NPs were wrapped by a more crystalline TiO_x diatomic layer and only Ti^{3+} were present in the inclusions [59].

(2) Intermetallic bonding. Tauster et al. suggested that intermetallic bonding was facilitated by the overlap of the d and empty d orbitals of the excess metal between the active component and the support [56]. An Au/ZnO catalyst reported by Chung et al. showed that Au-Zn interactions could be formed by treating Au/ZnO with oxygen at different temperatures by fine structure resolution of Au by EXAFS. The formation of Au-Zn bonds (similar to AuZn alloys) can be directly detected after reduction at 300 °C under hydrogen atmosphere [58]. The phenomenon of intermetallic bonding caused by SMSI can be a rational strategy for researchers to regulate the electronic structure of active components in OER catalysts. In response to the limitations of the conventional AEM and LOM evolutionary mechanisms on the performance as well as the stability of acidic OER catalysts, Lin et al. innovatively reported an OER electrocatalyst (Ru/MnO_2) with Ru atomic array patches supported on α-MnO_2. The OER catalytic mechanism of this catalyst involves only *O and *OH species as intermediates. This mechanism allows the direct coupling of O-O radicals to generate and precipitate O_2. Ru/MnO_2 exhibits high OER activity (161 mV@10 mA cm^{-2}) and excellent stability (minimal loss of activity after 200 h of operation) and is one of the best-performing catalysts available for acid-stable oxygen precipitation reactions.

(3) Modification of the adsorption characteristics of the catalytical active component. As early as 1982, Burch et al. found that the adsorption of H_2 by the catalyst material was substantially reduced after high temperature reduction of Ni/TiO_2 at 650 °C [63]. It has also been mentioned in the literature that O-SMSI and A-SMSI constructed by oxygen treatment and adsorbent induction lead to a significant reduction in the adsorption capacity of the material for small molecules such as CO and H_2 [59][64]. The property that SMSI can change the adsorption characteristics of

the material allows one to design SMSI to adjust the adsorption energy of the catalyst material for OER reactions on intermediates, thus improving the catalytic effect of the catalyst and even improving the stability of the catalyst. According to the OER volcanogram, tungsten oxide has a relatively weaker O-binding capacity than iridium oxide, and it is thus possible to coordinate the O-binding capacity by constructing a W-Ir dual active site on the catalyst [65]. However, the actual catalytic effect of tungsten oxide in acidic OER is not satisfactory, due to its degradation by intermediates in the OER reaction [66].

3.3. Strong Oxide-Support Interaction (SOSI)

Initially, the SMSI was primarily concerned with strong interactions between metal atoms and supports, but this was gradually extended to strong interactions between metal-containing species and supports [67]. The concept of SOSI was derived to better describe the strong interactions between oxides and supports in order to distinguish them from SMSI. In general, similar to those of SMSI, SOSI has the following effects.

(1) SOSI can redistribute electrons at the oxide-support interface and modulate the electronic properties of the catalytic active site. Niu et al. reported the synthesis of a RuO_2/(Co, Mn)$_3O_4$ nanocomposite. The introduction of manganese in Co_3O_4 resulted in the redistribution of support electrons. By XPS characterization, the scholars found that RuO_2/(Co, Mn)$_3O_4$ catalysts appeared as electron-rich Ru species. The adsorption of O on RuO_2/(Co, Mn)$_3O_4$ was weakened as the electronic properties changed, which resulted in the rate-determining step in the OER process, i.e., the formation of OOH*, being accelerated. This cost-effective catalyst (ultra-low Ru content of 2.51 wt%) requires an overpotential of only 270 mV to achieve a current density of 10 mA cm^{-2} with a mass activity nearly 69 times better than that of commercial RuO_2 (**Figure 3**) [68].

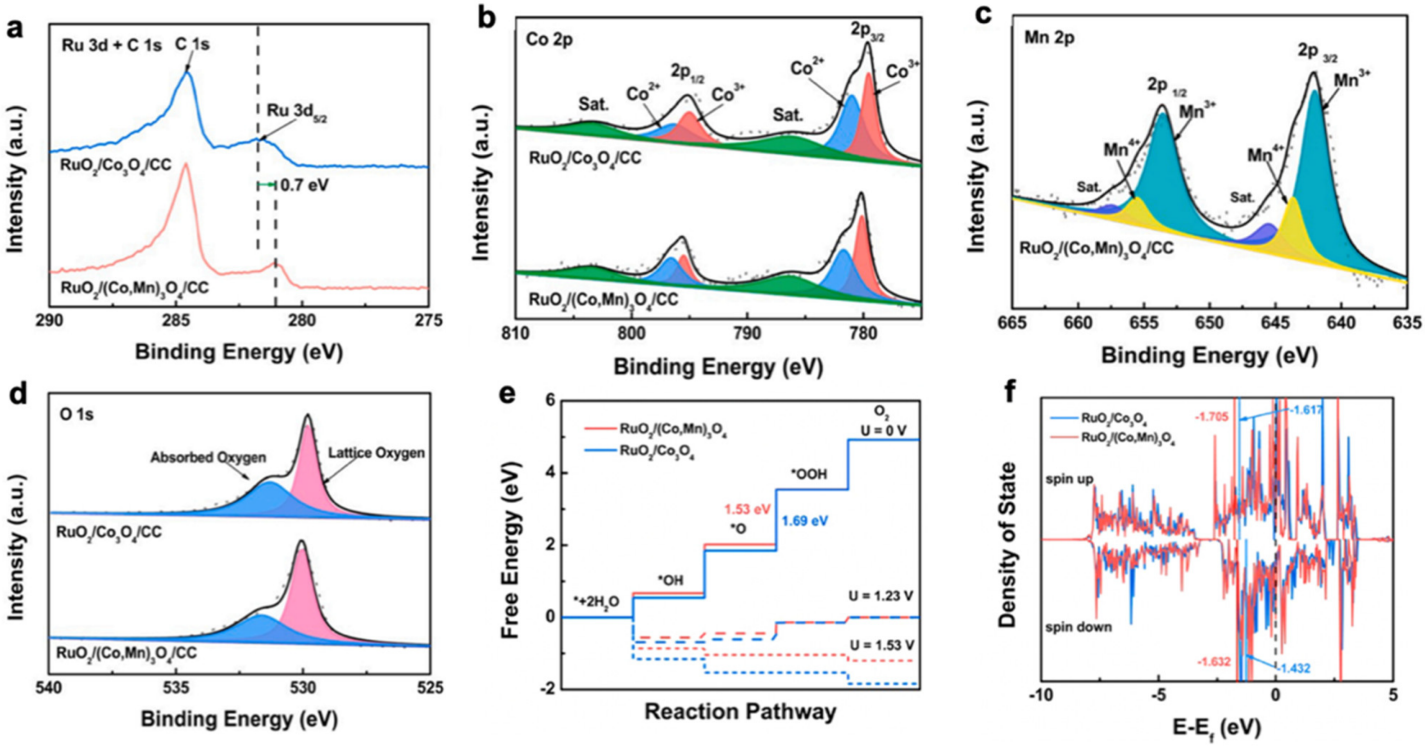

Figure 3. XPS spectra of (**a**) Ru 3d, (**b**) Co 2p, (**c**) Mn 2p, and (**d**) O 1s of RuO_2/Co_3O_4/CC and RuO_2/(Co, Mn)$_3O_4$/CC samples. (**e**) Gibbs free energy diagrams of supported catalysts. (**f**) Projected density of states (PDOS) of Ru d orbitals in supported catalysts [68].

(2) SOSI can also effectively reduce the aggregation of NPs in electrocatalytic reactions, thereby improving the atomic utilization and stability of the material. WC-loaded RuO_2 NPs (RuO_2-WC NPs) anchored on carbon nanosheets reported by Sun et al. exhibited strong catalyst-support interactions and the low loading of Ru (4.11 wt.%) significantly enhanced the acidic oxygen precipitation reaction activity. The 10 mA/cm^2 overpotential was 347 mV and the mass activity was eight times higher than that of commercial RuO_2. The excellent OER performance can be attributed to the catalyst-support interaction between RuO_2 and the WC support. Theoretical calculations show that the strong catalyst-support interaction between RuO_2 and WC supports optimizes the electronic structure around the Ru site, giving good adsorption energy for OER intermediates and thus reducing the reaction potential of the RDS.

(3) SOSI can improve the catalytic performance of OER catalytic materials by building rich interfaces, thus improving the catalytic performance of OER catalytic materials. Highly dispersed IrO_2 nanoclusters (~1 nm) loaded on porous V_2O_5 supports were successfully prepared by Zheng et al. using a MIL-88B(V) organometallic framework as a self-sacrificing template. Through detailed characterization and comparative experiments, the strong interaction between IrO_2 nanoclusters and V_2O_5 supports resulted in significant lattice distortion of IrO_2 nanoclusters, which facilitated the exposure of more unsaturated coordination active sites. At the same time, the strong electron transfer (electron transfer from Ir to V) at the interface between IrO_2 and V_2O_5 allows the IrO_2 active sites to act as electrophilic centers, weakening the adsorption of oxygen-containing intermediates. DFT calculations suggested that the SOSI effect alters the occupation number of Ir eg orbitals, lowering the *O to *OOH energy barrier and thus effectively promoting the reaction rate of water oxidation. As a result, the IrO_2/V_2O_5 catalyst exhibited excellent OER activity in different media, exhibiting not only an ultra-low OER overpotential of 266 mV at 10 mA/cm^2 but also a high-performance all-water decomposition over a wide pH range (**Figure 4**) [69].

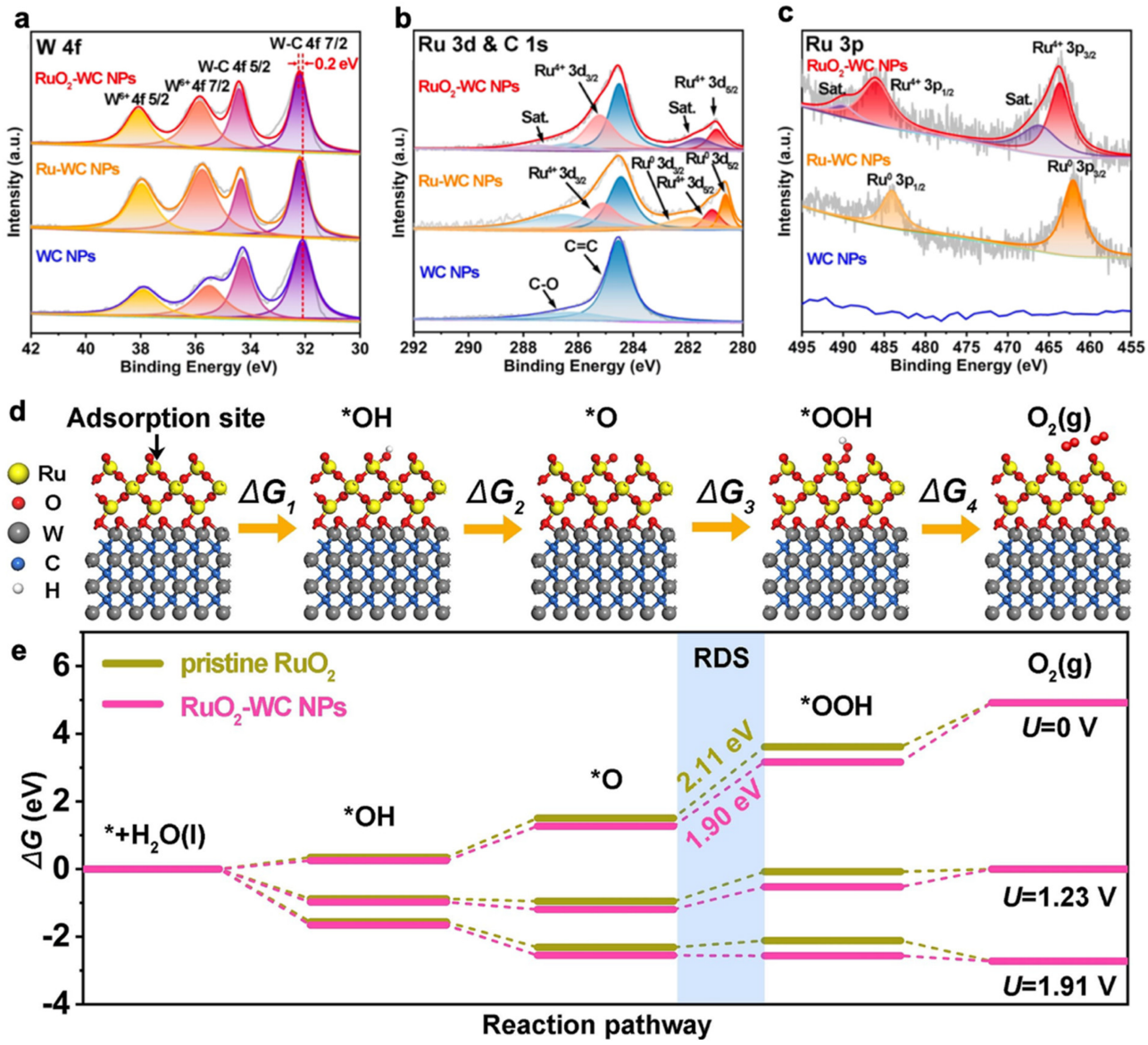

Figure 4. XPS spectra of RuO_2–WC NPs, Ru–WC NPs and WC NPs. High-resolution XPS spectra of (**a**) W 4f, (**b**) Ru 3d and C 1s, and (**c**) Ru 3p. (**d**) Mechanism of OER process steps and corresponding Gibbs free energies of reaction intermediates on RuO_2–WC NPs. (**e**) Free energy landscape of pristine RuO_2 and RuO_2–WC NPs at zero potential (U = 0), equilibrium potential (U = 1.23 V), and the potential (U = 1.91 V) for which each step is downhill of RuO_2–WC NPs, respectively [70].

3.4. Electron-Metal-Support Interactions (EMSI)

EMSI can lead to changes in the electronic structure of the metal particles and alter the adsorption and activation energies of reactant molecules, resulting in enhanced catalytic properties. In 2012, Campbell et al. first proposed electronic metal-support interactions (EMSI) based on the interaction between platinum and cerium atoms [71]. Specifically, EMSI refers to the charge redistribution phenomenon at the interface between the two, the support and the NPs, in a loaded metal nanoparticle catalyst. This is manifested as a local environmental change in the

metal site, causing a change in the d-band (ε_d) structure of the metal. By designing and modulating EMSI, the ε_d of the metal can be increased, thereby enhancing the catalytic performance of the catalyst [67][71].

Catalyst systems with typical EMSI effects have been identified: metal-doped carbon (M-dN), metal-transition metal compound groups (M-TMCs) and metal-metal substrates [67]. EMSI involves the formation of chemical bonds due to the mixing of metal d-orbitals. On the one hand, this interaction stabilizes the metal NPs; on the other hand, the support effect will greatly influence the catalytic performance of the metal NPs [72][73].The energy balance at the metal-support interface reduces the activation energy of the reaction and thus increases the catalytic activity of the catalyst. The electron flow at the metal-support interface is decisive for the Fermi energy balance of the catalyst [74]. The properties of the support, the loaded metal NPs, defects, and so on can influence the electron transfer process [53]. The net electron transfer across the metal-support interface enhances the chemisorption of the metal NPs to the reactants [75].

References

1. Eisenberg, R.; Gray, H.B.; Crabtree, G.W. Addressing the challenge of carbon-free energy. Proc. Natl. Acad. Sci. USA 2020, 117, 12543–12549.
2. Dincer, I.; Acar, C. Review and evaluation of hydrogen production methods for better sustainability. Int. J. Hydrogen Energy 2015, 40, 11094–11111.
3. Herron, J.A.; Kim, J.; Upadhye, A.A.; Huber, G.W.; Maravelias, C.T. A general framework for the assessment of solar fuel technologies. Energy Environ. Sci. 2015, 8, 126–157.
4. Feustel, J. Possibilities and limitations of wind energy utilisation. Int. J. Ambient. Energy 2011, 2, 197–205.
5. Fouz, D.M.; Carballo, R.; López, I.; Iglesias, G. Tidal stream energy potential in the Shannon Estuary. Renew. Energy 2022, 185, 61–74.
6. Nosratabadi, S.M.; Hemmati, R.; Bornapour, M.; Abdollahpour, M. Economic evaluation and energy/exergy analysis of PV/Wind/PEMFC energy resources employment based on capacity, type of source and government incentive policies: Case study in Iran. Sustain. Energy Technol. Assess. 2021, 43, 100963.
7. O'Connell, A.; Kelly, A.L.; Tobin, J.; Ruegg, P.L.; Gleeson, D. The effect of storage conditions on the composition and functional properties of blended bulk tank milk. J. Dairy Sci. 2017, 100, 991–1003.
8. Oetjen, H.F.; Schmidt, V.M.; Stimming, U.; Trila, F. Performance Data of a Proton Exchange Membrane Fuel Cell Using H2/CO as Fuel Gas. J. Electrochem. Soc. 1996, 143, 3838.

9. Zhao, Y.; Mao, Y.; Zhang, W.; Tang, Y.; Wang, P. Reviews on the effects of contaminations and research methodologies for PEMFC. Int. J. Hydrogen Energy 2020, 45, 23174–23200.
10. Balaji, R.; Senthil, N.; Vasudevan, S.; Ravichandran, S.; Mohan, S.; Sozhan, G.; Madhu, S.; Kennedy, J.; Pushpavanam, S.; Pushpavanam, M. Development and performance evaluation of Proton Exchange Membrane (PEM) based hydrogen generator for portable applications. Int. J. Hydrogen Energy 2011, 36, 1399–1403.
11. Carmo, M.; Fritz, D.L.; Mergel, J.; Stolten, D. A comprehensive review on PEM water electrolysis. Int. J. Hydrogen Energy 2013, 38, 4901–4934.
12. Chen, Y.; Liu, C.; Xu, J.; Xia, C.; Wang, P.; Xia, B.Y.; Yan, Y.; Wang, X. Key Components and Design Strategy for a Proton Exchange Membrane Water Electrolyzer. Small Struct. 2022, 27, 2200130.
13. Shiva Kumar, S.; Himabindu, V. Hydrogen production by PEM water electrolysis—A review. Mater. Sci. Energy Technol. 2019, 2, 442–454.
14. Fabbri, E.; Schmidt, T.J. Oxygen Evolution Reaction—The Enigma in Water Electrolysis. ACS Catal. 2018, 8, 9765–9774.
15. Gao, J.; Tao, H.; Liu, B. Progress of Nonprecious-Metal-Based Electrocatalysts for Oxygen Evolution in Acidic Media. Adv. Mater. 2021, 33, e2003786.
16. Song, J.; Wei, C.; Huang, Z.F.; Liu, C.; Zeng, L.; Wang, X.; Xu, Z.J. A review on fundamentals for designing oxygen evolution electrocatalysts. Chem. Soc. Rev. 2020, 49, 2196–2214.
17. Ma, Q.; Mu, S. Acidic oxygen evolution reaction: Mechanism, catalyst classification, and enhancement strategies. Interdiscip. Mater. 2023, 2, 53–90.
18. Shi, Z.; Wang, Y.; Li, J.; Wang, X.; Wang, Y.; Li, Y.; Xu, W.; Jiang, Z.; Liu, C.; Xing, W.; et al. Confined Ir single sites with triggered lattice oxygen redox: Toward boosted and sustained water oxidation catalysis. Joule 2021, 5, 2164–2176.
19. Xu, X.; Pan, Y.; Zhong, Y.; Shi, C.; Guan, D.; Ge, L.; Hu, Z.; Chin, Y.Y.; Lin, H.J.; Chen, C.T.; et al. New Undisputed Evidence and Strategy for Enhanced Lattice-Oxygen Participation of Perovskite Electrocatalyst through Cation Deficiency Manipulation. Adv. Sci. 2022, 9, e2200530.
20. Yoo, J.S.; Rong, X.; Liu, Y.; Kolpak, A.M. Role of Lattice Oxygen Participation in Understanding Trends in the Oxygen Evolution Reaction on Perovskites. ACS Catal. 2018, 8, 4628–4636.
21. Luo, R.; Qian, Z.; Xing, L.; Du, C.; Yin, G.; Zhao, S.; Du, L. Re-Looking into the Active Moieties of Metal X-ides (X-=Phosph-, Sulf-, Nitr-, and Carb-) Toward Oxygen Evolution Reaction. Adv. Funct. Mater. 2021, 31, 2102918.
22. Han, H.; Kim, I.; Park, S. Cobalt-based oxygen evolution catalyst as active and stable as iridium in acidic media. Electrochim. Acta 2020, 344, 136160.

23. Wen, Y.; Chen, P.; Wang, L.; Li, S.; Wang, Z.; Abed, J.; Mao, X.; Min, Y.; Dinh, C.T.; Luna, P.; et al. Highly Active Ru Sites by Suppressing Lattice Oxygen Participation in Acidic Water Oxidation. J. Am. Chem. Soc. 2021, 143, 6482–6490.
24. Liu, Z.; Liu, Y.; He, H.; Shao, H.; Zhang, Y.; Li, J.; Cai, W. Valence regulation of Ru/Mo2C heterojunction for efficient acidic overall water splitting. Electrochim. Acta 2023, 443, 141920.
25. Yao, Q.; Huang, B.; Xu, Y.; Li, L.; Shao, Q.; Huang, X. A chemical etching strategy to improve and stabilize RuO2-based nanoassemblies for acidic oxygen evolution. Nano Energy 2021, 84, 105909.
26. Guo, H.; Fang, Z.; Li, H.; Fernandez, D.; Henkelman, G.; Humphrey, S.M.; Yu, G. Rational Design of Rhodium-Iridium Alloy Nanoparticles as Highly Active Catalysts for Acidic Oxygen Evolution. ACS Nano 2019, 13, 13225–13234.
27. Li, H.; Liu, H.; Qin, Q.; Liu, X. BaLaIr double mixed metal oxides as competitive catalysts for oxygen evolution electrocatalysis in acidic media. Inorg. Chem. Front. 2022, 9, 702–708.
28. Ying, Y.; Godinez Salomon, J.F.; Lartundo-Rojas, L.; Moreno, A.; Meyer, R.; Damin, C.A.; Rhodes, C.P. Hydrous cobalt-iridium oxide two-dimensional nanoframes: Insights into activity and stability of bimetallic acidic oxygen evolution electrocatalysts. Nanoscale Adv. 2021, 3, 1976–1996.
29. Sharma, L.; Katiyar, N.K.; Parui, A.; Das, R.; Kumar, R.; Tiwary, C.S.; Singh, A.K.; Halder, A.; Biswas, K. Low-cost high entropy alloy (HEA) for high-efficiency oxygen evolution reaction (OER). Nano Res. 2021, 15, 4799–4806.
30. Zhao, J.-W.; Shi, Z.-X.; Li, C.-F.; Ren, Q.; Li, G.-R. Regulation of Perovskite Surface Stability on the Electrocatalysis of Oxygen Evolution Reaction. ACS Mater. Lett. 2021, 3, 721–737.
31. Liu, W.; Kawano, K.; Kamiko, M.; Kato, Y.; Okazaki, Y.; Yamada, I.; Yagi, S. Effects of A-site Cations in Quadruple Perovskite Ruthenates on Oxygen Evolution Catalysis in Acidic Aqueous Solutions. Small 2022, 18, e2202439.
32. Liang, X.; Shi, L.; Liu, Y.; Chen, H.; Si, R.; Yan, W.; Zhang, Q.; Li, G.D.; Yang, L.; Zou, X. Activating Inert, Nonprecious Perovskites with Iridium Dopants for Efficient Oxygen Evolution Reaction under Acidic Conditions. Angew. Chem. Int. Ed. Engl. 2019, 58, 7631–7635.
33. Chen, H.; Shi, L.; Sun, K.; Zhang, K.; Liu, Q.; Ge, J.; Liang, X.; Tian, B.; Huang, Y.; Shi, Z.; et al. Protonated Iridate Nanosheets with a Highly Active and Stable Layered Perovskite Framework for Acidic Oxygen Evolution. ACS Catal. 2022, 12, 8658–8666.
34. Zhang, T.; Zhang, B.; Peng, Q.; Zhou, J.; Sun, Z. Mo2B2 MBene-supported single-atom catalysts as bifunctional HER/OER and OER/ORR electrocatalysts. J. Mater. Chem. A 2021, 9, 433–441.
35. Cao, L.; Luo, Q.; Chen, J.; Wang, L.; Lin, Y.; Wang, H.; Liu, X.; Shen, X.; Zhang, W.; Liu, W.; et al. Dynamic oxygen adsorption on single-atomic Ruthenium catalyst with high performance for acidic

oxygen evolution reaction. Nat. Commun. 2019, 10, 4849.

36. Yin, J.; Jin, J.; Lu, M.; Huang, B.; Zhang, H.; Peng, Y.; Xi, P.; Yan, C.H. Iridium Single Atoms Coupling with Oxygen Vacancies Boosts Oxygen Evolution Reaction in Acid Media. J. Am. Chem. Soc. 2020, 142, 18378–18386.
37. Gao, Z.; Lai, Y.; Gong, L.; Zhang, L.; Xi, S.; Sun, J.; Zhang, L.; Luo, F. Robust Th-MOF-Supported Semirigid Single-Metal-Site Catalyst for an Efficient Acidic Oxygen Evolution Reaction. ACS Catal. 2022, 12, 9101–9113.
38. Li, S.; Gao, Y.; Li, N.; Ge, L.; Bu, X.; Feng, P. Transition metal-based bimetallic MOFs and MOF-derived catalysts for electrochemical oxygen evolution reaction. Energy Environ. Sci. 2021, 14, 1897–1927.
39. Singh, K.; Guillen Campos, J.d.J.; Dinic, F.; Hao, Z.; Yuan, T.; Voznyy, O. Manganese MOF Enables Efficient Oxygen Evolution in Acid. ACS Mater. Lett. 2020, 2, 798–800.
40. Li, Z.; Zou, J.; Liang, T.; Song, X.; Li, Z.; Wen, J.; Peng, M.; Zeng, X.; Huang, H.; Wu, H. MOF-derived ultrasmall 2 heterostructures as bifunctional and pH-universal electrocatalysts for 0.79 V asymmetric amphoteric overall water splitting. Chem. Eng. J. 2023, 460, 141672.
41. Patel, K.B.; Parmar, B.; Ravi, K.; Patidar, R.; Chaudhari, J.C.; Srivastava, D.N.; Bhadu, G.R. Metal-organic framework derived core-shell nanoparticles as high performance bifunctional electrocatalysts for HER and OER. Appl. Surf. Sci. 2023, 616, 156499.
42. Li, S.; Lei, X.; Hu, H.; Fu, L.; Peng, R.; Huang, H.; Wang, J. Flaky cobalt phosphide-modified manganese iron oxide as a highly efficient OER catalyst. New J. Chem. 2021, 45, 11797–11802.
43. Li, A.; Sun, Y.; Yao, T.; Han, H. Earth-Abundant Transition-Metal-Based Electrocatalysts for Water Electrolysis to Produce Renewable Hydrogen. Chemistry 2018, 24, 18334–18355.
44. Lin, Y.; Zhang, M.; Zhao, L.; Wang, L.; Cao, D.; Gong, Y. Ru doped bimetallic phosphide derived from 2D metal organic framework as active and robust electrocatalyst for water splitting. Appl. Surf. Sci. 2021, 536, 147952.
45. Zhou, Y.-N.; Yu, N.; Lv, Q.-X.; Liu, B.; Dong, B.; Chai, Y.-M. Surface evolution of Zn doped-RuO2 under different etching methods towards acidic oxygen evolution. J. Mater. Chem. A 2022, 10, 16193–16203.
46. Zhang, H.; Wu, B.; Su, J.; Zhao, K.; Chen, L. MOF-Derived Zinc-Doped Ruthenium Oxide Hollow Nanorods as Highly Active and Stable Electrocatalysts for Oxygen Evolution in Acidic Media. ChemNanoMat 2021, 7, 117–121.
47. Park, Y.J.; Lee, J.; Park, Y.S.; Yang, J.; Jang, M.J.; Jeong, J.; Choe, S.; Lee, J.W.; Kwon, J.D.; Choi, S.M. Electrodeposition of High-Surface-Area IrO2 Films on Ti Felt as an Efficient Catalyst for the Oxygen Evolution Reaction. Front. Chem. 2020, 8, 593272.

48. Gou, W.; Zhang, M.; Zou, Y.; Zhou, X.; Qu, Y. Iridium-Chromium Oxide Nanowires as Highly Performed OER Catalysts in Acidic Media. ChemCatChem 2019, 11, 6008–6014.
49. Liu, H.; Wang, Z.; Li, M.; Zhao, X.; Duan, X.; Wang, S.; Tan, G.; Kuang, Y.; Sun, X. Rare-earth-regulated Ru-O interaction within the pyrochlore ruthenate for electrocatalytic oxygen evolution in acidic media. Sci. China Mater. 2021, 64, 1653–1661.
50. Gao, L.; Zhong, X.; Chen, J.; Zhang, Y.; Liu, J.; Zhang, B. Optimizing the electronic structure of Fe-doped Co3O4 supported Ru catalyst via metal-support interaction boosting oxygen evolution reaction and hydrogen evolution reaction. Chin. Chem. Lett. 2022, 108085.
51. Karim, W.; Spreafico, C.; Kleibert, A.; Gobrecht, J.; VandeVondele, J.; Ekinci, Y.; van Bokhoven, J.A. Catalyst support effects on hydrogen spillover. Nature 2017, 541, 68–71.
52. Wurster, B.; Grumelli, D.; Hotger, D.; Gutzler, R.; Kern, K. Driving the Oxygen Evolution Reaction by Nonlinear Cooperativity in Bimetallic Coordination Catalysts. J. Am. Chem. Soc. 2016, 138, 3623–3626.
53. Pacchioni, G. Electronic interactions and charge transfers of metal atoms and clusters on oxide surfaces. Phys. Chem. Chem. Phys. 2013, 15, 1737–1757.
54. Zhang, B.; Qin, Y. Interface Tailoring of Heterogeneous Catalysts by Atomic Layer Deposition. ACS Catal. 2018, 8, 10064–10081.
55. Van Deelen, T.W.; Hernández Mejía, C.; de Jong, K.P. Control of metal-support interactions in heterogeneous catalysts to enhance activity and selectivity. Nat. Catal. 2019, 2, 955–970.
56. Tauster, S.J.; Fung, S.C.; Garten, R.L. Group 8 noble metals supported on TiO2. J. Am. Chem. Soc. 1978, 100, 100–175.
57. Xu, J.; Li, J.; Lian, Z.; Araujo, A.; Li, Y.; Wei, B.; Yu, Z.; Bondarchuk, O.; Amorim, I.; Tileli, V.; et al. Atomic-Step Enriched Ruthenium–Iridium Nanocrystals Anchored Homogeneously on MOF-Derived Support for Efficient and Stable Oxygen Evolution in Acidic and Neutral Media. ACS Catal. 2021, 11, 3402–3413.
58. Liu, X.; Liu, M.H.; Luo, Y.C.; Mou, C.Y.; Lin, S.D.; Cheng, H.; Chen, J.M.; Lee, J.F.; Lin, T.S. Strong metal-support interactions between gold nanoparticles and ZnO nanorods in CO oxidation. J. Am. Chem. Soc. 2012, 134, 10251–10258.
59. Matsubu, J.C.; Zhang, S.; DeRita, L.; Marinkovic, N.S.; Chen, J.G.; Graham, G.W.; Pan, X.; Christopher, P. Adsorbate-mediated strong metal-support interactions in oxide-supported Rh catalysts. Nat. Chem. 2017, 9, 120–127.
60. Dong, J.; Fu, Q.; Li, H.; Xiao, J.; Yang, B.; Zhang, B.; Bai, Y.; Song, T.; Zhang, R.; Gao, L.; et al. Reaction-Induced Strong Metal-Support Interactions between Metals and Inert Boron Nitride Nanosheets. J. Am. Chem. Soc. 2020, 142, 17167–17174.

61. Xu, W.; Huang, H.; Wu, X.; Yuan, Y.; Liu, Y.; Wang, Z.; Zhang, D.; Qin, Y.; Lai, J.; Wang, L. Mn-doped Ru/RuO2 with strong metal-support interaction for efficient water splitting in acidic media. Compos. Part B Eng. 2022, 242, 110013.
62. Tang, H.; Su, Y.; Zhang, B.; Lee, A.F.; Isaacs, M.A.; Wilson, K.; Li, L.; Ren, Y.; Huang, J.; Haruta, M.; et al. Classical strong metal–support interactions between gold nanoparticles and titanium dioxide. Sci. Adv. 2017, 3, e1700231.
63. Burch, R.; Flambard, A.R. Strong Metal-Support Interactions in Nickel/Titania Catalysts: The Importance of Interfacial Phenomena. J. Catal. 1982, 78, 389–405.
64. Jin, L.; Liu, B.; Louis, M.E.; Li, G.; He, J. Highly Crystalline Mesoporous Titania Loaded with Monodispersed Gold Nanoparticles: Controllable Metal-Support Interaction in Porous Materials. ACS Appl. Mater. Interfaces 2020, 12, 9617–9627.
65. Wu, J.; Liu, M.; Chatterjee, K.; Hackenberg, K.P.; Shen, J.; Zou, X.; Yan, Y.; Gu, J.; Yang, Y.; Lou, J.; et al. Exfoliated 2D Transition Metal Disulfides for Enhanced Electrocatalysis of Oxygen Evolution Reaction in Acidic Medium. Adv. Mater. Interfaces 2016, 3, 1500669.
66. Chakrapani, V.; Thangala, J.; Sunkara, M.K. WO3 and W2N nanowire arrays for photoelectrochemical hydrogen production. Int. J. Hydrogen Energy 2009, 34, 9050–9059.
67. Yang, J.; Li, W.; Wang, D.; Li, Y. Electronic Metal–Support Interaction of Single-Atom Catalysts and Applications in Electrocatalysis. Adv. Mater. 2020, 32, 2003300.
68. Niu, S.; Kong, X.-P.; Li, S.; Zhang, Y.; Wu, J.; Zhao, W.; Xu, P. Low Ru loading RuO2/(Co,Mn)3O4 nanocomposite with modulated electronic structure for efficient oxygen evolution reaction in acid. Appl. Catal. B Environ. 2021, 297, 120442.
69. Zheng, X.; Qin, M.; Ma, S.; Chen, Y.; Ning, H.; Yang, R.; Mao, S.; Wang, Y. Strong Oxide-Support Interaction over IrO2/V2 O5 for Efficient pH-Universal Water Splitting. Adv. Sci. 2022, 9, e2104636.
70. Sun, S.C.; Jiang, H.; Chen, Z.Y.; Chen, Q.; Ma, M.Y.; Zhen, L.; Song, B.; Xu, C.Y. Bifunctional WC-Supported RuO2 Nanoparticles for Robust Water Splitting in Acidic Media. Angew. Chem. Int. Ed. 2022, 61, e202202519.
71. Campbell, C.T. Catalyst-support interactions: Electronic perturbations. Nat. Chem. 2012, 4, 597–598.
72. Shi, Y.; Wang, J.; Wang, C.; Zhai, T.T.; Bao, W.J.; Xu, J.J.; Xia, X.H.; Chen, H.Y. Hot electron of Au nanorods activates the electrocatalysis of hydrogen evolution on MoS2 nanosheets. J. Am. Chem. Soc. 2015, 137, 7365–7370.
73. Lykhach, Y.; Kozlov, S.M.; Skala, T.; Tovt, A.; Stetsovych, V.; Tsud, N.; Dvorak, F.; Johanek, V.; Neitzel, A.; Myslivecek, J.; et al. Counting electrons on supported nanoparticles. Nat. Mater. 2016,

15, 284–288.

74. Losurdo, M.; Yi, C.; Suvorova, A.; Rubanov, S.; Kim, T.H.; Giangregorio, M.M.; Jiao, W.; Bergmair, I.; Bruno, G.; Brown, A.S. Demonstrating the Capability of the High-Performance Plasmonic Gallium–Graphene Couple. ACS Nano 2014, 8, 3031–3034.
75. Chen, G.; Xu, C.; Huang, X.; Ye, J.; Gu, L.; Li, G.; Tang, Z.; Wu, B.; Yang, H.; Zhao, Z.; et al. Interfacial electronic effects control the reaction selectivity of platinum catalysts. Nat. Mater. 2016, 15, 564–569.